Dispersion Corrected r^{2}SCAN Based Global Hybrid Functionals: r^{2}SCANh, r^{2}SCAN0, and r^{2}SCAN50

Markus Bursch,[1] Hagen Neugebauer,[2] Sebastian Ehlert,[2] and Stefan Grimme[2]
[1)] *Max-Planck-Institut für Kohlenforschung, Kaiser-Wilhelm-Platz 1, D-45470 Mülheim an der Ruhr, Germany*
[2)] *Mulliken Center for Theoretical Chemistry, Universität Bonn, Beringstr. 4, D-53115 Bonn, Germany*

(*Electronic mail: grimme@thch.uni-bonn.de)

(*Electronic mail: bursch@kofo.mpg.de)

(Dated: 21 January 2022)

The re-regularized semilocal meta generalized gradient approximation (meta-GGA) exchange-correlation functional r^{2}SCAN [J. W. Furness, A. D. Kaplan, J. Ning, J. P. Perdew, and J. Sun, J. Phys. Chem. Lett. 11, 8208–8215 (2020)] is used to create three global hybrid functionals with varying admixtures of Hartree–Fock "exact" exchange (HFX). The resulting functionals r^{2}SCANh (10% HFX), r^{2}SCAN0 (25% HFX), and r^{2}SCAN50 (50% HFX) are combined with the semi-classical D4 London dispersion correction. The new functionals are assessed for the calculation of molecular geometries, main-group, and metalorganic thermochemistry at 26 comprehensive benchmark sets. These include the extensive GMTKN55 database, ROST61, and IONPI19 sets. It is shown that a moderate admixture of HFX leads to relative improvements of the mean absolute deviations (MADs) for thermochemistry of 11% (r^{2}SCANh-D4), 16% (r^{2}SCAN0-D4), and 1% (r^{2}SCAN50-D4) compared to the parental semi-local meta-GGA. For organometallic reaction energies and barriers, r^{2}SCAN0-D4 yields an even larger mean improvement of 35%. The computation of structural parameters (geometry optimization) does not systematically profit from HFX admixture. Overall, the best variant r^{2}SCAN0-D4 performs well for both main-group and organometallic thermochemistry and is better or on par with well-established global hybrid functionals such as PW6B95-D4 or PBE0-D4. Regarding systems prone to self-interaction errors (SIE4x4), r^{2}SCAN0-D4 shows reasonable performance, reaching the quality of the range-separated ωB97X-V functional. Accordingly, r^{2}SCAN0-D4 in combination with a sufficiently converged basis set (def2-QZVP(P)) represents a robust and reliable choice for general use in the calculation of thermochemical properties of both, main-group and organometallic chemistry.

I. INTRODUCTION

In the last decades, Kohn–Sham density functional theory (DFT) has emerged as a versatile and powerful tool in quantum chemistry.[1] DFT has proven to provide broad applicability towards a large variety of chemical problems at a typically excellent computational cost accuracy ratio. This has led to its status as the "working horse" of quantum chemistry and caused a massive impulse in the development of new density functional approximations (DFAs). These are usually categorized according to the "Jacob's ladder" hierarchy coined by Perdew and Schmidt in 2001.[2] The introduced rungs reflect the respective methodological improvement of DFAs, resulting in categories of local (spin-)density approximations (LDAs), generalized gradient approximations (GGAs), meta-GGAs, hybrid functionals, and double-hybrid functionals. Even though the expected accuracy of the DFAs improves ascending the rungs of Jacob's ladder, this also results in increasing computational demand. While (meta-)GGA functionals formally scale cubic with the system size (N^3), hybrid DFAs already have a formal scaling of N^4 due to the admixture of Hartree-Fock "exact" exchange (HFX) into the energy calculation. Nevertheless, for the less computationally demanding (meta-)GGA functionals the self-interaction error (SIE) is specifically problematic for the calculation of, e.g., reaction barriers. The admixture of HFX in hybrid functionals reduces the impact from SIE and therefore typically improves results for systems prone to this kind of error. Here, hybrid functionals can be classified into global hybrid functionals, applying a fixed HFX parameter, and range-separated hybrid (RSH) functionals that divide the Coulomb operator into short- and long-ranged regimes that apply different fractions of HFX. Even though RSH functionals address overdelocalization effects in the long-ranged regime more accurately compared to global hybrid functionals,[3] the robustness and computational efficiency of the latter render them still highly valuable in most quantum chemical applications. Successful variants are the well-known PBE0, PW6B95, and TPSSh hybrid functionals. An interesting starting point for the development of new global hybrid functionals is the strongly constrained and appropriately normed (SCAN) functional[4] as it is constructed to rigorously satisfy all known exact constraints applicable to a meta-GGA. Previously proposed global hybrid functionals, like SCANh[5] (10% HFX) and SCAN0[6] (25% HFX), were developed without any correction for London dispersion interactions, which cannot be included by semilocal functionals,[7] and therefore are not competitive for real chemical applications. Martin and Santra[8] developed dispersion corrected global hybrid SCAN functionals with 10%, 25%, 37.5%, and 50% by utilizing the D4 dispersion correction[9]. One major shortcoming inherited from the SCAN functional for those hybrid functionals are the severe numerical instabilities and the resulting need to use dense computationally costly integration grids,[10–12] which impedes their application for many computational studies. This issue is resolved with the regularized SCAN (rSCAN)[11] and the subsequent r^{2}SCAN functional.[12,13] Inspired by the excellent performance of r^{2}SCAN, its London dispersion corrected variants,[14] and the composite DFT method r^{2}SCAN-3c,[15] we present three global hybrid functional variants of r^{2}SCAN termed r^{2}SCANh, r^{2}SCAN0, and r^{2}SCAN50 with 10%, 25%, and 50% of HFX admixture, respectively. Matching parameters for the D4,[9,16] the D3(BJ),[17,18] and the non-self consistent VV10[19] London dispersion correction are provided. To provide a clear picture of the capabilities of the new functionals, their performance is assessed for a variety of state-of-the-art benchmark data. These include thermochemistry, kinetics, non-covalent interactions, and molecular geometries of main-group elements (*e.g.* GMTKN55,[20] IONPI19[21]) and transition metal compounds (*e.g.* MOR41,[22] ROST61[23]).

II. METHODS

A. Hartree–Fock exchange admixture

The recently proposed re-regularized SCAN meta-GGA exchange-correlation functional is modified by admixture of varied amounts of HFX. The obtained global hybrid exchange-correlation functionals are constructed according to equation 1 with a denoting the factor of HFX.

$$E_{xc}^{\mathrm{r^2SCAN}x} = (1-a)E_X^{\mathrm{r^2SCAN}} + aE_X^{\mathrm{HF}} + E_C^{\mathrm{r^2SCAN}} \tag{1}$$

In this work we present three variants with increasing amounts of HF exchange admixture. Referring to the well known TPSSh/0, PBE0, and BHLYP hybrid functionals, the proposed exchange correlation functionals are r^{2}SCANh (10%), r^{2}SCAN0 (25%), and r^{2}SCAN50 (50%). No re-parameterization of the original r^{2}SCAN functional was conducted.

B. Dispersion corrections

In general, the application of London dispersion corrections has proven indispensable.[7,24,25] Therefore, the recently developed atomic-charge dependent London dispersion correction D4[9,16] was parameterized for the new hybrid functionals. In the D4 correction scheme, the dispersion energy is calculated according to equation (2) including an Axilrod–Teller–Muto (ATM) type three-body energy correction.

$$E_{disp}^{D4} = -\frac{1}{2}\sum_{AB}\sum_{n=6,8} s_n \frac{C_{(n)}^{AB}}{R_{AB}^{(n)}} f_{damp}^{(n)}(R_{AB}) \tag{2a}$$

$$-\frac{1}{6}\sum_{ABC} s_9 \frac{C_{(9)}^{ABC}}{R_{ABC}^{(9)}} f_{damp}^{(9)}(R_{ABC}, \theta_{ABC}) \tag{2b}$$

where $A/B/C$ are the atomic indices, R_{AB} their distance, $C_{(n)}^{AB}$ is the nth dispersion coefficient and θ_{ABC} the angle dependent term of the atomic triple. The default Becke–Johnson (BJ) damping function $f_{BJ}^{(n)}(R_{AB})$ is applied as described in equation (3).

$$f_{BJ}^{(n)}(R_{AB}) = \frac{R_{AB}^{(n)}}{R_{AB}^{(n)} + (a_1 R_0^{AB} + a_2)^{(n)}} \tag{3}$$

For a detailed description of the D4 correction see references 9 and 16. Accordingly, the D4 model requires three functional specific parameters s_8, a_1, and a_2. The newly determined parameters for D4 as well as D3(BJ) and the parameter b for a non-self-consistent VV10 dispersion correction are are presented in table I.

C. Parameterization strategy

Independently from this work, Santra and Martin[26] proposed a number of density corrected hybrids based on r^{2}SCAN and have provided D4 parameters for those methods. The major difference in the parameterization strategy employed by Santra and Martin is the use of the GMTKN55 set and the WTMAD-2 as objective function, while we followed the proven original parameterization strategy proposed in Ref. 9, which minimizes the mean-square deviation for non-covalent interaction curves. Furthermore, since the interaction curves are not counter–poise corrected, the residual basis set superposition error can be accounted for in the damping parameters, especially for the triple-ζ basis sets. We prefer this strategy to provide a targeted correction of London dispersion effects and to avoid overfitting by including systems prone to various other error sources such as the self-interaction error (SIE) in the SIE4x4 subset of the GMTKN55. The resulting parameters differ significantly, especially in the value of the s_8 dipole–quadrupole scaling. While Santra and Martin reported values around three for the s_8, we found smaller and more physical values < 1, which is in line with previous parameterizations of the rational damping function for SCAN[10] and r^{2}SCAN.[14] To investigate the effect of this discrepancy we evaluated all benchmark sets tested for this work with the parameters proposed by Santra and Martin as well.

Unsurprisingly, we find that the damping parameters proposed by Santra and Martin perform slightly better by 0.2 kcal·mol^{-1} for the GMTKN55, as this was the objective function for optimizing the damping parameters. However, we find that damping parameters optimized on the GMTKN55 will produce spurious interaction energies for large molecule benchmark sets with large dispersion contributions such as the S30L set increasing the MAD by 2.4 kcal·mol^{-1} for r^{2}SCAN0-D4 with the damping parameters by Santra and Martin. For most sets tested in this study both damping parameters yield similar results in the MAD. However, the benefit in the improved WTMAD-2 is out-weighted by the deterioration in interaction energies for large systems. Further, the tendentially smaller mean deviations using our parameterizations hint on a more systematic correction of the descriptions of London dispersion effects for the r^{2}SCANx hybrid functionals. For completeness we included a full statistics of the

TABLE I. Presented hybrid exchange-correlation functionals, HFX admixture, and determined parameters for the D4, D3(BJ), and VV10 London dispersion corrections fit for def2-QZVP (QZ) and def2-TZVPP (TZ) basis sets.

		D4 / QZ					D3(BJ) / QZ					VV10 / QZ
Functional	HFX	s_6	s_8	s_9	a_1	a_2	s_6	s_8	s_9	a_1	a_2	b
r^{2}SCANh	10%	1	0.8324	1	0.4944	5.9019	1	1.1236	1	0.4709	5.9157	11.9
r^{2}SCAN0	25%	1	0.8992	1	0.4778	5.8779	1	1.1846	1	0.4534	5.8972	11.4
r^{2}SCAN50	50%	1	1.0471	1	0.4574	5.8969	1	1.3294	1	0.4311	5.9240	10.8
		D4 / TZ					D3(BJ) / TZ					VV10 / TZ
Functional	HFX	s_6	s_8	s_9	a_1	a_2	s_6	s_8	s_9	a_1	a_2	b
r^{2}SCANh	10%	1	0.9119	1	0.4832	6.2073	1	1.1493	1	0.4761	6.0947	-
r^{2}SCAN0	25%	1	0.9397	1	0.4578	6.1864	1	1.1859	1	0.4567	6.0583	-
r^{2}SCAN50	50%	1	1.0576	1	0.4232	6.2378	1	1.2980	1	0.4314	6.0662	-

Santra and Martin damping parameters for all tested sets in the supporting information.

D. Computational details

All quantum chemical calculations were conducted with the `ORCA` 5.0.1 program package.[27,28] DFT calculations were generally accelerated using the resolution-of-the-identity approximation[29,30] for Coulomb and exchange integrals (RIJK) applying matching auxiliary basis sets[31,32] (*def2/JK* option). If not stated else, Ahlrichs' type large quadruple-ζ def2-QZVP and def2-QZVPP basis sets[33] were applied in the following abbreviated as "QZ". Triple-ζ basis set calculations employ the def2-TZVPP basis set abbreviated by "TZ." For all basis sets, the default Stuttgart–Dresden small-core effective core potentials[34,35] (ECPs) were used for the respective elements. The numerical quadrature grid option *DefGrid3* and *TightSCF* convergence criteria were generally applied as implemented in `ORCA`. D4 London dispersion corrections were calculated with the `dftd4` 3.3.0 stand-alone program.

III. RESULTS AND DISCUSSION

A. Main-group thermochemistry

To evaluate the performance of the proposed global hybrid DFAs for general main group chemistry, we employ the general thermochemistry, kinetics and noncovalent interactions (GMTKN55) database.[20] The GMTKN55 database is a compilation of 55 benchmark sets and comprises 1505 relative energies divided into five categories, namely, basic properties and reactions of small systems (basic properties), isomerisations and reactions of large systems (reactions), barrier heights (barriers), intermolecular noncovalent interactions (intermol. NCIs), and intramolecular noncovalent interactions (intramol. NCIs). The comparison between r^{2}SCAN and its hybrid variants, as well as the comparison of r^{2}SCAN0-D4 to other very well performing hybrid DFAs over the five categories as well as their weighted MAD (WTMAD-2) are shown in Figure 1. The global hybrid r^{2}SCAN DFAs yield smaller WTMAD-2 values than the meta-GGA with r^{2}SCAN0-D4 as their best performer (WTMAD-2 = 5.64 kcal·mol^{-1}), which is an improvement of almost 2 kcal·mol^{-1} over r^{2}SCAN-D4. The other two global hybrid DFAs r^{2}SCANh-D4 and r^{2}SCAN50-D4 perform slightly worse with WTMAD-2s of 6.23 kcal·mol^{-1} and 6.28 kcal·mol^{-1} respectively. The largest improvements with the inclusion of HFX, and therefore the reduction of SIE, are observed for barriers, while the remaining four categories benefit moderately from HFX. For the basic properties the improvements for the self-interaction error related problems (SIE4x4) set with HFX are compensated by the worse performance for total atomisation energies (W4-11). In comparison of r^{2}SCAN0-D4 with the well-performing hybrid functionals PBE0-D4, PW6B95-D4, and ωB97X-V, the r^{2}SCAN0-D4 outperforms PBE0-D4 (WTMAD-2 = 6.66 kcal·mol^{-1}), is on par with PW6B95-D4 (WTMAD-2 = 5.53 kcal·mol^{-1}), and performs moderately worse than the computationally more demanding RSH ωB97X-V (WTMAD-2 = 3.98 kcal·mol^{-1}).

Reducing the applied basis set to triple-ζ quality (def2-TZVPP) leads to moderate increases in the WTMAD-2 values of 4 (r^{2}SCAN50-D4 to 9% (r^{2}SCANh-D4, r^{2}SCAN0-D4).

B. Non-covalent interactions

Noncovalent interactions are of crucial importance in many chemical systems. Therefore, all hybrids were assessed on various benchmark sets representing diverse NCI patterns. These include NCIs of large systems (S30L, L7), ion-π interactions (IONPI19[21]), halogen bonds (X40x10[36]), hydrogen bonds (HB300SPX[37]), chalcogen bonds (CHAL336[38]), and NCIs in repulsive regions (R160x6[39,40]). Further, the subsets of the GMTKN55[20] that involve significant influence of intramolecular (IDISP, ICONF, ACONF, Amino20x4, PCONF21, MCONF, SCONF, UPU23, BUT14DIOL) and intermolecular NCIs (RG18, ADIM6, S22, S66, HEAVY28, WATER27, CARBHB12, PNICO23, HAL59, AHB21, CHB6, IL16) were assessed. The results of the proposed hybrid DFAs is depicted in Figure 2. Finally, a comparison of r^{2}SCAN0-D4 to other very well performing DFAs is shown in Figure 3.

For the calculation of NCIs, the correct description of London dispersion effects is indispensable.[7,24] Accordingly, the

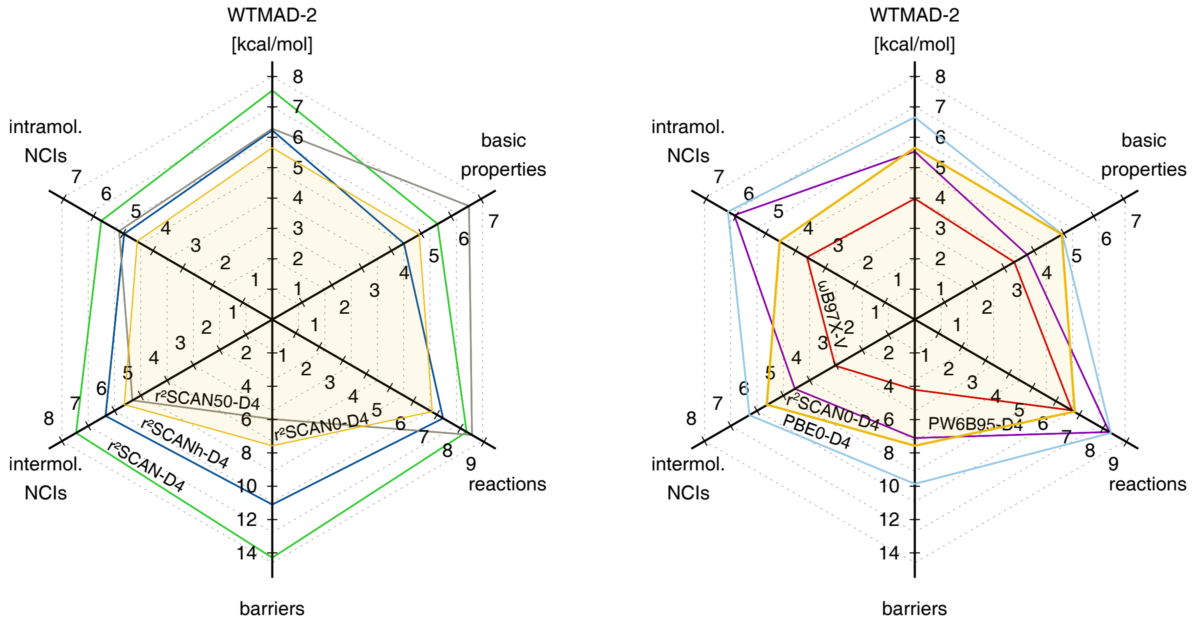

FIG. 1. Weighted mean absolute deviation of r^{2}SCANx-D4 hybrids compared to other very well performing DFAs for the large database of general main group thermochemistry, kinetics and non-covalent interactions GMTKN55. On the left side panel the different r^{2}SCANx-D4 hybrids are compared against the meta-GGA r^{2}SCAN-D4.

parameterization of sophisticated dispersion corrections such as the D4 method to systematically correct DFT and in this case the r^{2}SCANx hybrid functionals is specifically crucial. The r^{2}SCANx-D4 hybrid functionals with moderate amounts of HFX (10, 25%) yield systematically improved results for NCIs compared to the pure meta-GGA. For r^{2}SCAN0-D4, the MAD for the NCI subsets of the GMTKN55, is reduced from 0.83 kcal·mol^{-1} to 0.62 kcal·mol^{-1}, which is an improvement of 25%. Further, the description of hydrogen bonds (HB300SPX) is improved, reducing the MAD from 0.62 kcal·mol^{-1} to 0.53 kcal·mol^{-1}. On average r^{2}SCAN0-D4 yields an improvement of 8% for NCIs. Tentatively, this positive effects of HFX admixture can be attributed to a reduced SIE leading to smaller artificial intramolecular charge-transfer. Large amounts of HFX on the other hand, lead to increased errors for some subsets such as the L7 and IONPI19 benchmark sets with increased MAD by 17% compared to r^{2}SCAN-D4. No improvement for any of the tested hybrid functionals is observed for the S30L and X40x10 (halogen bonds) benchmark sets, yet retaining the already excellent performance of the meta-GGA. Overall, the description of NCIs by the r^{2}SCANx hybrid functionals in combination with the D4 correction is on par with other very well performing global hybrid functionals such as PW6B95-D4. The excellent results obtained with the RSH ωB97X-V are not reached by any of the assessed hybrid variants. Also for NCIs the def2-TZVPP yields comparably good results for most subsets compared to a QZ quality basis set. Nevertheless, NCIs proved to be the most basis set sensitive subgroup assessed with percent increases in the MADs of up to 70% (r^{2}SCANh-D4, IONPI19) relative to the QZ value. All MAD increases due to basis set size reduction are still below 0.7 kcal·mol^{-1}. Suprisingly, for the S30L even a small improvement of the MADs applying the def2-TZVPP basis set was observed (approx. -0.15 kcal·mol^{-1}).

C. Organometallic thermochemistry

All hybrid functionals were assessed in the context of the thermochemistry of organometallic complexes. Reaction energies were assessed for closed-shell transition metal complexes on the comprehensive MOR41[22] and WCCR10[42,43] benchmark sets and for open-shell transition metal complexes on the ROST61[23] benchmark set. Reaction barrier heights of transition metal complex reactions are represented by the MOBH35[44,45] and a collection of 34 barrier heights computed by Chen and co-workers termed TMBH.[46–49] Further, the MLA24 represents a collection of alkylchains linked by a (earth) alkaline or transition metal.[50] A comparison of the obtained results to the parent r^{2}SCAN meta-GGA functional is depicted in Figure 2. For all sets, small to moderate admixture of HFX (10%, 25%) results in smaller deviations and reduced error scattering. While 25% HFX admixture (r^{2}SCAN0) yields the best overall results, a further HFX increase to 50% (r^{2}SCAN50) increases the deviations significantly. This is in line with previous observations on increased errors upon inclusion of high amounts of HFX in the context of transition metal thermochemistry.[22,23] The frequently used M06-2X functional applying 54% HFX, shows a similar behavior compared to its sibling M06 (27%). Also, admixture of 25% HFX has proven very successful in the PBE0 functional.[51] A

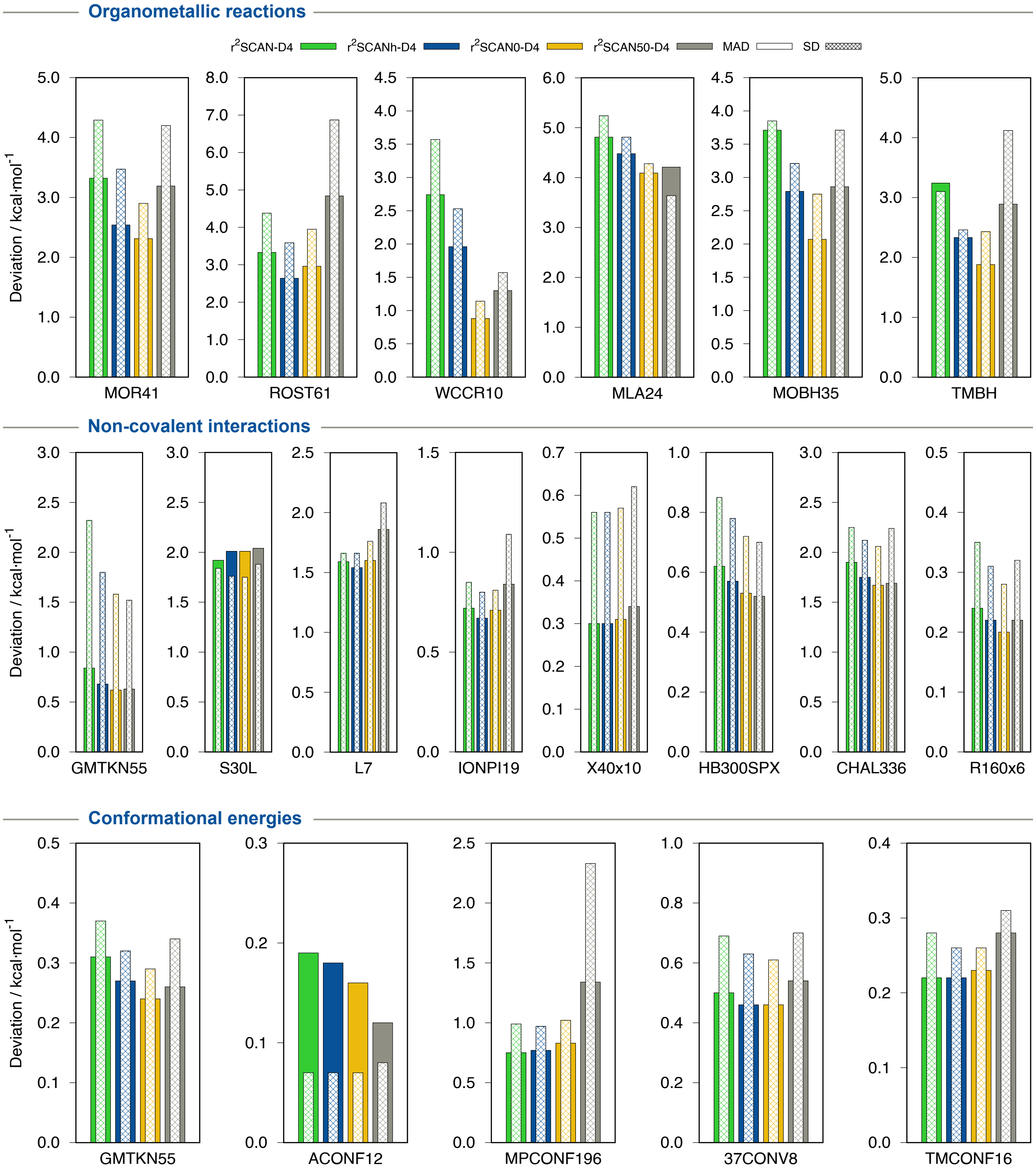

FIG. 2. Box-plots of deviations (MAD, SD) for organometallic reactions, non-covalent interactions, and conformational energies obtained with r^{2}SCAN-D4/QZ and its r^{2}SCANx-D4/QZ hybrid (x = h, 0, 50) variants. All deviations are given in kcal·mol^{-1}.

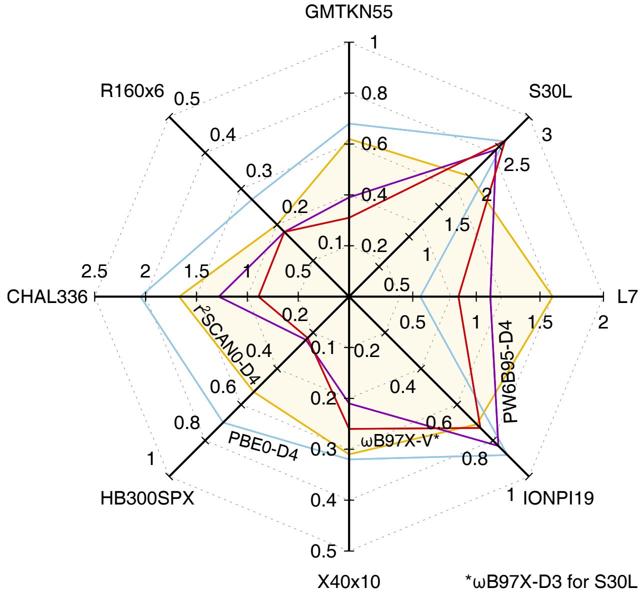

FIG. 3. Radar chart of the MADs for r^{2}SCAN0-D4 in comparison to other very well performing (RS-)hybrid DFAs. For different non-covalent interaction benchmark sets. Data for S30L was taken from Ref. 41.

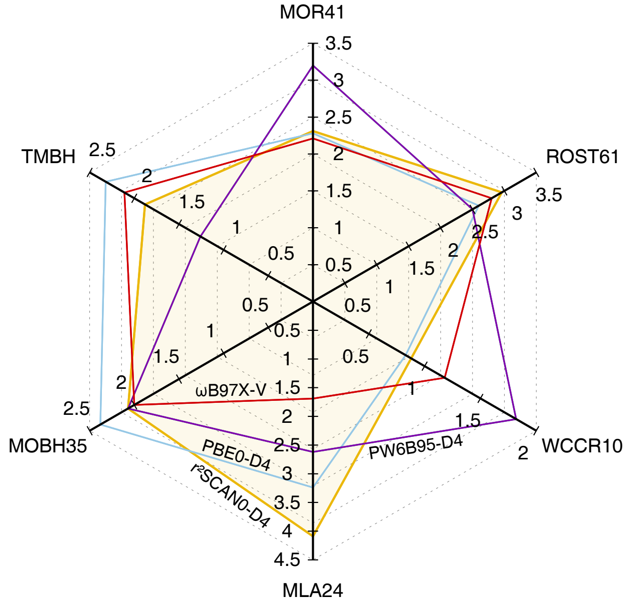

FIG. 4. Radar chart of the MADs for r^{2}SCAN0-D4 in comparison to other very well performing (RS-)hybrid DFAs for different metalorganic benchmark sets.

large improvement of the hybrid approach over the original meta-GGA is observed for the reaction barrier height subsets MOBH35 and TMBH overall decreasing the respective MADs by 44 and 42% for r^{2}SCAN0-D4. In general, specifically the r^{2}SCAN0-D4 functional reliably yields good results for transition metal complex thermochemistry. For the MOR41 benchmark set, r^{2}SCAN0-D4 is only outperformed by the range-separated ωB97X-V (MAD = 2.21 kcal·mol^{-1}) and the PWPB95-D3(BJ) (MAD = 1.85 kcal·mol^{-1}) double-hybrid functional.[22] For the ROST61, containing challenging open-shell single-reference complexes, it yields a good MAD of 2.96 kcal·mol^{-1}which is close to that of ωB97X-V (MAD = 2.8).[23] An even better performance is observed for the WCCR10 benchmark set, where r^{2}SCAN0-D4 yields a very small MAD of only 0.88 kcal·mol^{-1}, which is similar to the best tested DFA PBE0 that yields a MAD of 0.83 kcal·mol^{-1} in combination with the D4 dispersion correction. For all subsets covering organometallic chemistry, also reasonable MADs can be obtained from applying the smaller def2-TZVPP basis set. The resulting MAD increases are typically below 0.2 kcal·mol^{-1}.

D. Conformational energies

The reliable computation of conformational energies is of high importance in many quantum chemical applications as finding the energetically most favored conformer is fundamental.[52] Moreover, many properties require the consideration of well described conformer-ensembles that may be generated by sophisticated conformer-ensemble sampling algorithms such as CREST.[53] The final energetic ranking of conformers often requires more accurate methods, that still keep a beneficial cost-accuracy ratio. Accordingly, the application of global hybrid functionals may be desired. The performance of the r^{2}SCANx functionals for computation of conformational energies was assessed for various conformational energy benchmarks sets. These include the MPCONF196, the 37CONF8, the ACONF12, and the corresponding subsets of the GMTKN55 for main group conformers. Further, the TMCONF16 addresses conformational energies in transition metal complexes. Results are depicted in Figure 2. A comparison of r^{2}SCAN0-D4 to other very well performing DFAs is shown in Figure 5. While reaction energies and barriers were shown to profit greatly from moderate HFX admixture in the framework of r^{2}SCANx global hybrid functionals, no significant improvement is observed for conformational energies. While conformational energies of alkanes (ACONF12) are improved by 5, 16, and 37%, respectively, no systematic improvement is observed for (bio-)chemically relevant molecules covered by the MPCONF196 and 37CONF8 or the transition metal complexes of the TMCONF16. Nevertheless, it is to note, that the differences in the MADs compared to r^{2}SCAN-D4 are typically very small and below 0.1 kcal·mol^{-1}. Overall specifically r^{2}SCAN0-D4 yields excellent conformational energies mostly on par with the RSH ωB97X-V. Except for the ACONF12 benchmark set, the results for conformational energies are quite insensitive to the reduction in basis set size from QZ to TZ.

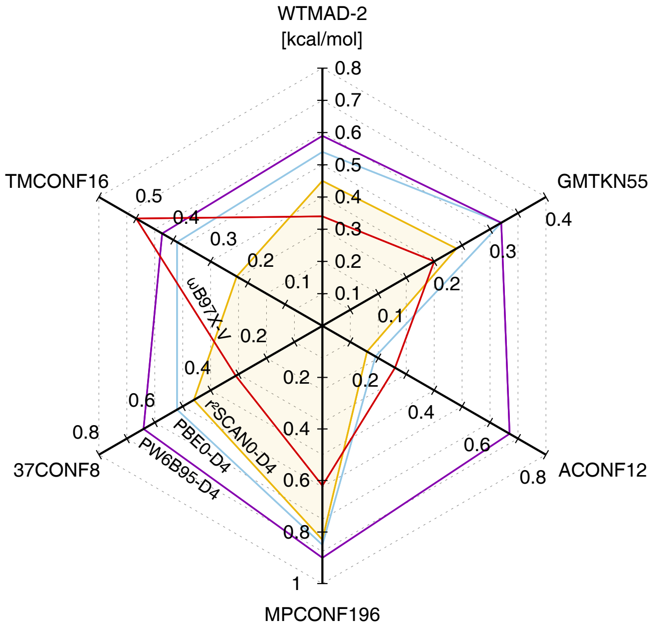

FIG. 5. Radar chart of the MADs for r^{2}SCAN0-D4 in comparison to other very well performing (RS-)hybrid DFAs for different conformational benchmark sets.

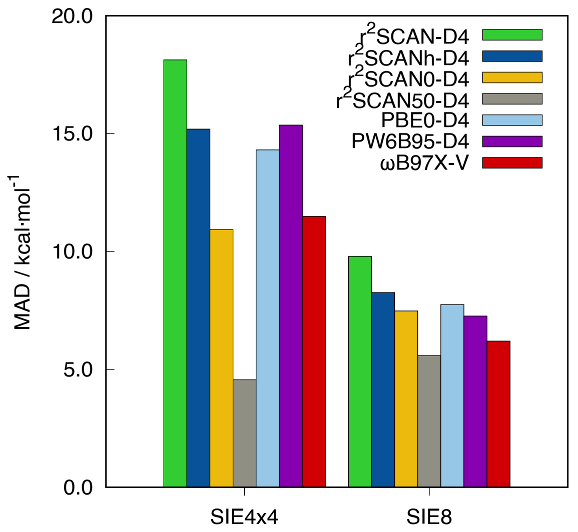

FIG. 6. MADs for the SIE4x4 and SIE8 sets. All DFT data calculated with the def2-QZVPP basis set.

E. Self-interaction Error

The artificial interaction of an electron with its own mean field is one of the major shortcomings of common KS-DFT. The so-called self-interaction error (SIE)[54–56] is specifically problematic in any local density functional approximation and in part also in various hybrid functionals. Accordingly, also the parental r^{2}SCAN meta-GGA functional is prone to SIE. Even though, several approaches to correct the SIE are known[57] the most common one is to introduce HFX in the hybrid DFT scheme. Therefore, the hybrid variants of r^{2}SCAN should show an improved performance for SIE prone systems and properties. The improvement of HFX inclusion regarding the SIE was assessed for the SIE4x4 and SIE8 subsets. The SIE4x4 subset of the GMTKN55 includes dissociation energies of small open-shell cationic dimers and the SIE8 consists of the remaining mostly neutral systems of the original SIE11 subset presented in the GMTKN24[58] database. The results for the r^{2}SCAN*x*-D4 hybrid functionals are depicted in Figure 6. For all three hybrids, a substantial improvement is observed for both subsets dependent on the amount of HFX admixture. With respect to the meta-GGA r^{2}SCAN-D4 (MAD = 18.1 kcal·mol^{-1}), the MAD is reduced to 15.2 kcal·mol^{-1}for r^{2}SCANh-D4 (10% HFX), to 10.9 kcal·mol^{-1} for r^{2}SCAN0-D4 (25% HFX), and to 4.6 kcal·mol^{-1} for r^{2}SCAN50 (50% HFX). A comparable improvement is observed for the SIE8 subset, where the MAD is reduced from 9.8 kcal·mol^{-1} (r^{2}SCAN-D4), to 8.3, 7.5, and 5.6 kcal·mol^{-1}, respectively. Even though the 50% HFX variant yields the smallest MADs for both subsets and also outperforms sophisticated DFAs such as the range-separated ωB97X-V functional[59], the high amount of HFX has proven not beneficial for the overall performance as discussed in the previous sections. However, the best tested compromise r^{2}SCAN0-D4 with 25% HFX yields reasonable results on par with ωB97X-V and even outperforms the prominent PBE0-D4 global hybrid functional. The influence of SIE was further evaluated for a system of the IONPI19[21] benchmark set, involving the non-covalent interaction energy of the cyclopropylium cation and anthracene (Figure 7). The interaction energy scan of both unrelaxed fragments along with the center-of-mass distance (R$_{CMA}$) was analyzed with reference to W1-F12 data. Here, a similar trend regarding the HFX admixture is observed as the interaction energy curve increasingly approaches the reference data. Nevertheless, for r^{2}SCAN50-D4, a beginning shift of the minimum value to a larger R$_{CMA}$ is observed. While this is only indicated by a slight change in the shape of the curve for r^{2}SCAN50-D4, ωB97X-V already yields a different minimum R$_{CMA}$. Further, ωB97X-V systematically underestimates the interaction energy at shorter distances. Overall, it is shown that the HFX admixture to r^{2}SCAN-D4 significantly reduces the SIE as already indicated by the much improved performance for reaction barriers (*vide infra*). 25% HFX can be considered as the most promising compromise regarding the overall performance.

F. Geometries

In addition to thermochemical properties, the correct description of molecular geometries is of major interest. Specifically, covalent bond lengths and angles are key structural features. Accordingly, we assessed ground-state equilibrium distances (R_e) for transition metal complexes (TMC32[60]) and heavy and light main group compounds (HMGB11[61],

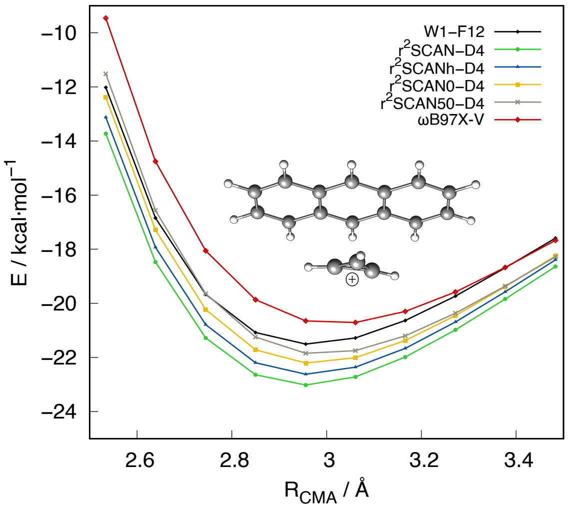

FIG. 7. Interaction energy scan of the cyclopropenyl cation and anthracene along the center-of-mass distance R$_{CMA}$. All DFT data calculated with the def2-QZVPP basis set.

LMGB35[61], LB12[61]). Further, distances and angles in organic molecules are compared to semi-experimental reference data (CCse21[62,63]). A comparison of r^{2}SCAN-D4/QZ and its hybrid variants is depicted in Figure 8. For geometries, an admixture of HFX did not prove beneficial regarding the reproduction of structural parameters. Mostly, the r^{2}SCANx-D4 hybrids yield slightly worse results compared to the already very well performing r^{2}SCAN-D4.[14] In the context of the higher computational demand of the hybrid functionals, geometry optimizations using such may not be recommended if no strong SIE effects are expected. Alternatively, the original r^{2}SCAN-D4 or its even more efficient composite variant r^{2}SCAN-3c[15] may be applied instead.

All collected MADs for all assessed thermochemistry and geometry benchmark sets are depicted in Table II.

IV. CONCLUSION

In this study global hybrid variants of the r^{2}SCAN meta-GGA functional are assessed on a large collection of comprehensive benchmark sets such as the GMTKN55, MOR41, HB300SPX, and CHAL336 data collections (overall about 6975 relative energies and 252 structural parameters in total). The used benchmark sets cover main-group and transition metal thermochemistry, non-covalent interactions and conformational energies. Starting from r^{2}SCAN, three different hybrid functionals with varying amounts of HFX admixture are constructed. The new global hybrid functionals are termed r^{2}SCANh (10% HFX), r^{2}SCAN0 (25%), and r^{2}SCAN50 (50%). The sophisticated D4 London dispersion correction is parameterized for all three hybrid functionals and an additional parameter set for use with a smaller triple-ζ basis set (def2-TZVPP) is provided. Additionally, we extensively tested the D4 damping parameters proposed by Santra and Martin for the r^{2}SCAN hybrids, which perform similarly well over a wide range of assessed benchmark sets. Nevertheless, the herein presented parameterization yields more systematic and consistent improvements indicated by reduced mean deviations and the absence of crucial outliers, specifically for dispersion dominated test sets such as the S30L.

It is shown that admixture of moderate amounts of HFX to r^{2}SCAN is beneficial for most assessed properties. For the GMTKN55 database, r^{2}SCAN0-D4/QZ yields a WTMAD-2 of 5.64 kcal·mol^{-1} compared to 7.54 kcal·mol^{-1} obtained with the parent r^{2}SCAN-D4/QZ meta-GGA. The same holds for organometallic reactions and reaction barrier heights, where small MADs of 2.31 kcal·mol^{-1} (MOR41) and 2.07 kcal·mol^{-1} (MOBH35) are obtained with r^{2}SCAN0-D4/QZ. Large amounts of 50% HFX were found to be beneficial only in very specific cases such as SIE prone systems covered by the SIE4x4 and SIE8 subsets.

For geometry optimization, no benefit of applying any r^{2}SCANx-D4 hybrid variant over the parent r^{2}SCAN-D4 meta-GGA was observed. In general, while the admixture of pure HFX proved beneficial, it yields comparably minor improvements for an already excellent performing and robust meta-GGA functional such as r^{2}SCAN. Therefore, the global r^{2}SCAN0-D4 hybrid functional applying 25% of HFX has proven to perform best regarding its broad applicability. It performs robustly for a variety of properties on par with other excellent performing functionals such as PW6B95-D4 and typically outperforms the prominent non-empirical PBE0-D4 functional. Because the underlying r^{2}SCAN functional remains unchanged, it can be expected that the potential energy surface is similar to that of r^{2}SCAN-D4 and r^{2}SCAN-3c making it a robust choice for multi-level protocols based on those functionals. Accordingly, the assessed r^{2}SCAN0-D4 global hybrid functional represent an efficient alternative to the still slightly more accurate RSH functionals such as ωB97X-V. It may be applied whenever the RSH cannot be applied due to technical reasons

Overall, r^{2}SCAN0-D4 can be considered as robust and reliable choice for a variety of computational chemistry applications.

ACKNOWLEDGMENTS

The German Science Foundation (DFG) is gratefully acknowledged for financial support (Grant 1927/16-1). Further, financial support by the "Sigrid-Peyerimhoff Forschungspreis" awarded to M. B. is acknowledged. We further thank Martin Blaško and Prof. Miroslav Urban for providing support with the MLA24 benchmark.

DATA AVAILABILITY

The data that support the findings of this study are openly available at `https://github.com/haneug/r2scanx-D4`.

[1] W. Kohn, "Nobel lecture: Electronic structure of matter—wave functions and density functionals," Reviews of Modern Physics **71**, 1253 (1999).

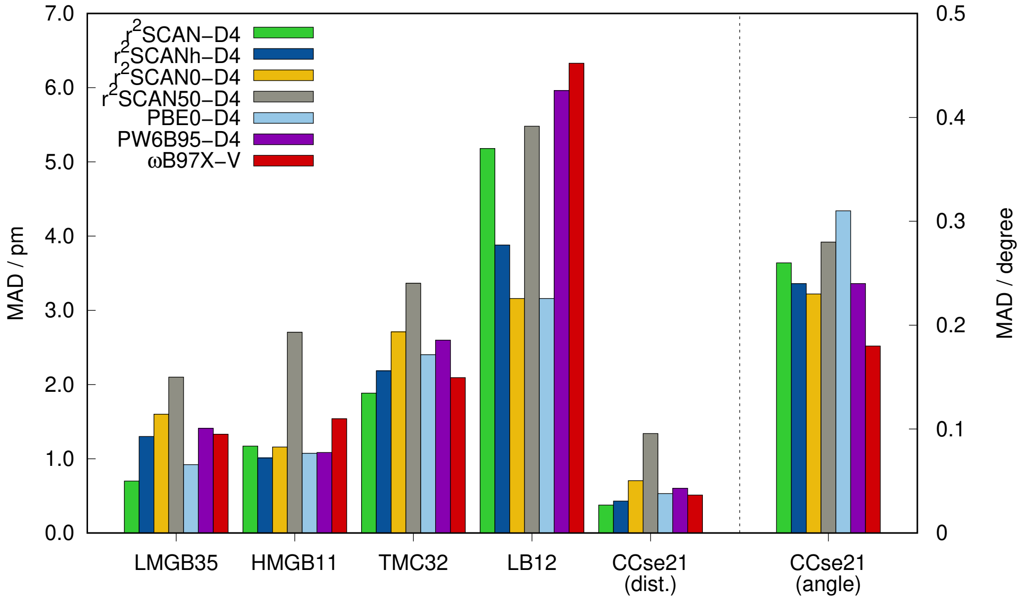

FIG. 8. Mean absolute deviations for geometries obtained with r^{2}SCAN-D4/QZ and its r^{2}SCANx-D4/QZ hybrid (x = h, 0, 50) variants compared to well-performing (RS-)hybrids. All deviations for bond lengths are given in pm, all for angles in degrees.

[2]J. P. Perdew and K. Schmidt, "Jacob's ladder of density functional approximations for the exchange-correlation energy," AIP Conf. Proc. **577**, 1–20 (2001).

[3]É. Brémond, Á. J. Pérez-Jiménez, J. C. Sancho-García, and C. Adamo, "Range-separated hybrid density functionals made simple," J. Chem. Phys. **150**, 201102 (2019).

[4]J. Sun, A. Ruzsinszky, and J. P. Perdew, "Strongly constrained and appropriately normed semilocal density functional," Phys. Rev. Lett. **115**, 036402 (2015).

[5]B. Chan, "Assessment and development of dft with the expanded cuagau-2 set of group-11 cluster systems," International Journal of Quantum Chemistry **121**, e26453 (2021), https://onlinelibrary.wiley.com/doi/pdf/10.1002/qua.26453.

[6]K. Hui and J.-D. Chai, "Scan-based hybrid and double-hybrid density functionals from models without fitted parameters," The Journal of Chemical Physics **144**, 044114 (2016), https://doi.org/10.1063/1.4940734.

[7]S. Grimme, A. Hansen, J. G. Brandenburg, and C. Bannwarth, "Dispersion-Corrected Mean-Field Electronic Structure Methods," Chem. Rev. **116**, 5105–5154 (2016).

[8]G. Santra and J. M. Martin, "What types of chemical problems benefit from density-corrected dft? a probe using an extensive and chemically diverse test suite," Journal of Chemical Theory and Computation **17**, 1368–1379 (2021), pMID: 33625863, https://doi.org/10.1021/acs.jctc.0c01055.

[9]E. Caldeweyher, S. Ehlert, A. Hansen, H. Neugebauer, S. Spicher, C. Bannwarth, and S. Grimme, "A generally applicable atomic-charge dependent London dispersion correction," Journal of Chemical Physics **150**, 154122 (2019).

[10]J. G. Brandenburg, J. E. Bates, J. Sun, and J. P. Perdew, "Benchmark tests of a strongly constrained semilocal functional with a long-range dispersion correction," Phys. Rev. B **94**, 115144 (2016).

[11]A. P. Bartók and J. R. Yates, "Regularized scan functional," The Journal of Chemical Physics **150**, 161101 (2019), https://doi.org/10.1063/1.5094646.

[12]J. W. Furness, A. D. Kaplan, J. Ning, J. P. Perdew, and J. Sun, "Accurate and Numerically Efficient r2SCAN Meta-Generalized Gradient Approximation," J. Phys. Chem. Lett. **11**, 8208–8215 (2020), 2008.03374.

[13]J. W. Furness, A. D. Kaplan, J. Ning, J. P. Perdew, and J. Sun, "Erratum: Accurate and Numerically Efficient r2SCAN Meta-Generalized Gradient Approximation (J. Phys. Chem. Lett. (2020) 11:19 (8208-8215) DOI: 10.1021/acs.jpclett.0c02405)," J. Phys. Chem. Lett. , 9248 (2020).

[14]S. Ehlert, U. Huniar, J. Ning, J. W. Furness, J. Sun, A. D. Kaplan, J. P. Perdew, and J. G. Brandenburg, "r2SCAN-D4: Dispersion corrected meta-generalized gradient approximation for general chemical applications," J. Chem. Phys. **154**, 061101 (2021), 2012.09249.

[15]S. Grimme, A. Hansen, S. Ehlert, and J.-M. Mewes, "r2SCAN-3c: A "Swiss army knife" composite electronic-structure method," J. Chem. Phys. **154**, 064103 (2021).

[16]E. Caldeweyher, C. Bannwarth, and S. Grimme, "Extension of the D3 dispersion coefficient model," J. Chem. Phys. **147**, 034112 (2017).

[17]S. Grimme, J. Antony, S. Ehrlich, and H. Krieg, "A consistent and accurate ab initio parametrization of density functional dispersion correction (dft-d) for the 94 elements h-pu," J. Chem. Phys. **132**, 154104 (2010).

[18]S. Grimme, S. Ehrlich, and L. Goerigk, "Effect of the damping function in dispersion corrected density functional theory," J. Comput. Chem. **32**, 1456–1465 (2011).

[19]O. A. Vydrov and T. Van Voorhis, "Nonlocal van der Waals density functional: The simpler the better," J. Chem. Phys. **133**, 244103 (2010), 1009.1421.

[20]L. Goerigk, A. Hansen, C. Bauer, S. Ehrlich, A. Najibi, and S. Grimme, "A look at the density functional theory zoo with the advanced GMTKN55 database for general main group thermochemistry, kinetics and noncovalent interactions," Phys. Chem. Chem. Phys. **19**, 32184–32215 (2017).

[21]S. Spicher, E. Caldeweyher, A. Hansen, and S. Grimme, "Benchmarking London dispersion corrected density functional theory for noncovalent ion-π interactions," Phys. Chem. Chem. Phys. **23**, 11635–11648 (2021).

[22]S. Dohm, A. Hansen, M. Steinmetz, S. Grimme, and M. P. Checinski, "Comprehensive Thermochemical Benchmark Set of Realistic Closed-Shell Metal Organic Reactions," J. Chem. Theory COmput **14**, 2596–2608 (2018).

[23]L. R. Maurer, M. Bursch, S. Grimme, and A. Hansen, "Assessing Density Functional Theory for Chemically Relevant Open-Shell Transition Metal Reactions," J. Chem. Theory Comput **17**, 6134–6151 (2021).

[24]M. Bursch, E. Caldeweyher, A. Hansen, H. Neugebauer, S. Ehlert, and S. Grimme, "Understanding and Quantifying London Dispersion Effects in Organometallic Complexes," Acc. Chem. Res. **52**, 258–266 (2019).

[25]D. J. Liptrot and P. P. Power, "London dispersion forces in sterically crowded inorganic and organometallic molecules," Nat. Rev. Chem. **1**, 1–12 (2017).

[26]G. Santra and J. M. Martin, "Pure and hybrid scan, rscan, and r2scan: Which one is preferred in ks-and hf-dft calculations, and how does d4 dispersion correction affect this ranking?" Molecules **27**, 141 (2022).

[27]F. Neese, "Software update: the orca program system, version 4.0," Wiley Interdiscip. Rev. Comput. Mol. Sci. **8**, e1327 (2018).

TABLE II. Mean absolute deviations (MADs) / standard deviations (SDs) for the r^2SCAN-D4 and its hybrid variants in kcal·mol^{-1}. All values for def2-QZVP(P) basis set with D4 dispersion correction if not noted otherwise.

Benchmark	r^2SCAN	r^2SCANh	r^2SCAN0	r^2SCAN50	ωB97X-V	PBE0	PW6B95
transition metal chemistry							
MOR41	3.32	2.54 / 3.47	2.31 / 2.90	3.19 / 4.20	2.21	2.28	3.20
ROST61	3.33	2.64 / 3.59	2.96 / 3.95	4.84 / 6.87	2.8	2.6	2.5
WCCR10	2.74	1.96 / 2.53	0.88 / 1.14	1.30 / 1.57	1.18	0.83	1.82
MOBH35	3.71	2.79 / 3.21	2.07 / 2.75	2.86 / 3.71	2.00	2.38	2.07
TMBH	3.24	2.33 / 2.46	1.88 / 2.43	2.89 / 4.12	2.11	2.32	1.26
MLA24	4.81	4.48 / 4.81	4.09 / 4.28	4.21 / 3.64	1.69	3.24	2.62
non-covalent interactions							
GMTKN55[a]	7.54	6.23 / —	5.64 / —	6.28 / —	3.98	6.66	5.53
L7	1.59	1.54 / 1.66	1.60 / 1.76	1.86 / 2.08	0.86	1.56	1.11
S30L	1.92	2.01 / 1.76	2.01 / 1.75	2.04 / 1.88	2.6[b]	2.59	2.45
IONPI19	0.72	0.67 / 0.80	0.71 / 0.81	0.84 / 1.09	0.73	0.88	0.83
X40x10	0.30	0.30 / 0.56	0.31 / 0.57	0.34 / 0.62	0.26	0.32	0.21
R160x6	0.24	0.22 / 0.31	0.20 / 0.28	0.22 / 0.32	0.18	0.27	0.18
HB300SPX	0.62	0.57 / 0.78	0.53 / 0.72	0.52 / 0.70	0.23	0.70	0.24
SIE8[c]	9.79	8.26 / 8.15	7.48 / 7.23	5.58 / 7.06	6.20	7.75	7.26
CHAL336	1.90	1.75 / 2.12	1.67 / 2.06	1.69 / 2.24	0.89	2.05	1.28
conformational energies							
ACONF12	0.19	0.18 / 0.07	0.16 / 0.07	0.12 / 0.08	0.26	0.19	0.67
MPCONF196	0.75	0.77 / 0.97	0.83 / 1.02	1.34 / 2.33	0.62	0.85	0.90
37CONF8	0.50	0.46 / 0.63	0.46 / 0.61	0.54 / 0.70	0.31	0.52	0.64
TMCONF16	0.22	0.22 / 0.26	0.23 / 0.26	0.28 / 0.31	0.50	0.39	0.43
structural parameters							
LMGB35	0.68	1.29 / 2.30	1.59 / 2.28	2.09 / 2.45	0.92	1.41	1.33
HMGB11	1.17	1.01 / 1.21	1.16 / 1.06	2.71 / 1.15	1.07	1.09	1.54
TMC32	1.89	2.18 / 1.80	2.71 / 1.96	3.37 / 2.73	2.40	2.60	2.09
ROT34	4.64	3.00 / 3.94	10.46 / 7.40	24.15 /16.28	3.86	11.71	7.71
LB12	3.57	3.88 / 5.77	3.16 / 5.05	5.48 / 9.14	3.16	5.96	6.33
CCse21 (dist.)	0.38	0.43 / 0.57	0.70 / 0.71	1.34 / 1.02	0.53	0.60	0.51
CCse21 (angles)	0.26	0.24 / 0.29	0.23 / 0.28	0.28 / 0.38	0.31	0.24	0.18

[a] WTMAD-2 calculated according to ref. 20. For detailed statistics on specific subsets see the SI.

[b] ωB97X-D3

[c] Remaining reactions of the original SIE subset of the GMTKN24. All other reactions are covered by the new SIE4x4 subset of the GMTKN55.

[28] ORCA – an ab initio, density functional and semiempirical program package, V. 5.0.1, F. Neese, MPI für Kohlenforschung, Mülheim a. d. Ruhr (Germany), **2021**.

[29] O. Vahtras, J. Almlöf, and M. W. Feyereisen, “Integral approximations for lcao-scf calculations,” Chem. Phys. Lett. **213**, 514–518 (1993).

[30] R. A. Kendall and H. A. Früchtl, “The impact of the resolution of the identity approximate integral method on modern ab initio algorithm development,” Theor. Chem. Acc. **97**, 158–163 (1997).

[31] K. Eichkorn, F. Weigend, O. Treutler, and R. Ahlrichs, “Auxiliary basis sets for main row atoms and transition metals and their use to approximate coulomb potentials,” Theor. Chem. Acc. **97**, 119–124 (1997).

[32] F. Weigend, “Accurate Coulomb-fitting basis sets for H to Rn,” Phys. Chem. Chem. Phys. **8**, 1057–1065 (2006).

[33] F. Weigend and R. Ahlrichs, “Balanced basis sets of split valence, triple zeta valence and quadruple zeta valence quality for H to Rn: Design and assessment of accuracy,” Phys. Chem. Chem. Phys. **7**, 3297 (2005).

[34] D. Andrae, U. Häußermann, M. Dolg, H. Stoll, and H. Preuß, “Energy-adjusted ab initio pseudopotentials for the second and third row transition elements,” Theor. Chim. Acta **77**, 123–141 (1990).

[35] K. A. Peterson, D. Figgen, E. Goll, H. Stoll, and M. Dolg, “Systematically convergent basis sets with relativistic pseudopotentials. II. Small-core pseudopotentials and correlation consistent basis sets for the post-*d* group 16–18 elements,” J. Chem. Phys. **119**, 11113–11123 (2003).

[36] M. K. Kesharwani, D. Manna, N. Sylvetsky, and J. M. Martin, “The X40×10 Halogen Bonding Benchmark Revisited: Surprising Importance of (n-1)d Subvalence Correlation,” J. Phys. Chem. A **122**, 2184–2197 (2018).

[37] J. Řezáč, “Non-Covalent Interactions Atlas Benchmark Data Sets 2: Hydrogen Bonding in an Extended Chemical Space,” J. Chem. Theory Comput. **16**, 6305–6316 (2020).

[38] N. Mehta, T. Fellowes, J. M. White, and L. Goerigk, “CHAL336 Benchmark Set: How Well Do Quantum-Chemical Methods Describe Chalcogen-Bonding Interactions?” J. Chem. Theory Comput. **17**, 2783–2806 (2021).

[39] V. M. Miriyala and J. Řezáč, “Testing Semiempirical Quantum Mechanical Methods on a Data Set of Interaction Energies Mapping Repulsive Contacts in Organic Molecules,” J. Phys. Chem. A **122**, 2801–2808 (2018).

[40] V. M. Miriyala and J. Řezáč, “Correction to: Testing semiempirical QM methods on a data set of interaction energies mapping repulsive contacts in organic molecules (Journal of Physical Chemistry A (2018) 122 :10 (2801–2808) DOI: 10.1021/acs.jpca.8b00260),” J. Phys. Chem. A **122**, 9585–9586 (2018).

[41] R. Sure and S. Grimme, “Comprehensive Benchmark of Association (Free) Energies of Realistic Host–Guest Complexes,” J. Chem. Theory Comput. **11**, 3785–3801 (2015).

[42] T. Husch, L. Freitag, and M. Reiher, “Calculation of Ligand Dissociation Energies in Large Transition-Metal Complexes,” J. Chem. Theory Comput. **14**, 2456–2468 (2018), 1801.06584.

[43] T. Husch, L. Freitag, and M. Reiher, “Erratum: Calculation of ligand dissociation energies in large transition-metal complexes (Journal of Chemical Theory and Computation (2018) 14:5 (2456–2468) DOI: 10.1021/acs.jctc.8b00061),” J. Chem. Theory Comput. **15**, 4295–4296 (2019).

[44] M. A. Iron and T. Janes, “Evaluating Transition Metal Barrier Heights with the Latest Density Functional Theory Exchange-Correlation Functionals: The MOBH35 Benchmark Database,” J. Phys. Chem. A **123**, 3761–3781 (2019).

[45] M. A. Iron and T. Janes, “Correction to ”Evaluating Transition Metal Barrier Heights with the Latest Density Functional Theory Exchange-Correlation Functionals: The MOBH35 Benchmark Database”,” J. Phys. Chem. A **2019**, 3761–3781 (2019).

[46] Y. Sun and H. Chen, “Performance of Density Functionals for Activation Energies of Re-Catalyzed Organic Reactions,” J. Chem. Theory Comput. **10**, 579–588 (2014).

[47] Y. Sun and H. Chen, “Performance of density functionals for activation energies of Zr-mediated reactions,” J. Chem. Theory Comput. **9**, 4735–4743 (2013).

[48] Y. Sun, L. Hu, and H. Chen, “Comparative Assessment of DFT Performances in Ru- and Rh-Promoted σ-Bond Activations,” J. Chem. Theory Comput **11**, 1428–1438 (2015).

[49] L. Hu and H. Chen, “Assessment of DFT Methods for Computing Activation Energies of Mo/W-Mediated Reactions,” J. Chem. Theory Comput. **11**, 4601–4614 (2015).

[50] M. Blaško, L. F. Pašteka, and M. Urban, “Dft functionals for modeling of polyethylene chains cross-linked by metal atoms. dlpno–ccsd(t) benchmark calculations,” The Journal of Physical Chemistry A **125**, 7382–7395 (2021).

[51] C. Adamo and V. Barone, “Toward reliable density functional methods without adjustable parameters: The PBE0 model,” J. Chem. Phys. **110**, 6158–6170 (1999), arXiv:1011.1669v3.

[52] S. Grimme, F. Bohle, A. Hansen, P. Pracht, S. Spicher, and M. Stahn, “Efficient quantum chemical calculation of structure ensembles and free energies for nonrigid molecules,” J. Phys. Chem. A **125**, 4039–4054 (2021).

[53] P. Pracht, F. Bohle, and S. Grimme, “Automated exploration of the low-energy chemical space with fast quantum chemical methods,” Phys. Chem. Chem. Phys. **22**, 7169–7192 (2020).

[54] J. P. Perdew and A. Zunger, “Self-interaction correction to density-functional approximations for many-electron systems,” Phys. Rev. B **23**, 5048–5079 (1981).

[55] P. Mori-Sánchez, A. J. Cohen, and W. Yang, “Many-electron self-interaction error in approximate density functionals,” J. Chem. Phys. **125**, 201102 (2006).

[56] J. L. Bao, L. Gagliardi, and D. G. Truhlar, “Self-Interaction Error in Density Functional Theory: An Appraisal,” J. Phys. Chem. Lett. **9**, 2353–2358 (2018).

[57] T. Tsuneda and K. Hirao, “Self-interaction corrections in density functional theory,” J. Chem. Phys. **140**, 18A513 (2014).

[58] L. Goerigk and S. Grimme, “A general database for main group thermochemistry, kinetics, and noncovalent interactions - Assessment of common and reparameterized (meta-)GGA density functionals,” J. Chem. Theory Comput. **6**, 107–126 (2010).

[59] N. Mardirossian and M. Head-Gordon, “wB97X-V: A 10-parameter, range-separated hybrid, generalized gradient approximation density functional with nonlocal correlation, designed by a survival-of-the-fittest strategy,” Phys. Chem. Chem. Phys. **16**, 9904–9924 (2014).

[60] M. Bühl and H. Kabrede, “Geometries of transition-metal complexes from density-functional theory,” J. Chem. Theory Comput. **2**, 1282–1290 (2006).

[61] S. Grimme, J. G. Brandenburg, C. Bannwarth, and A. Hansen, “Consistent structures and interactions by density functional theory with small atomic orbital basis sets,” J. Chem. Phys. **143**, 054107 (2015).

[62] M. Piccardo, E. Penocchio, C. Puzzarini, M. Biczysko, and V. Barone, “Semi-Experimental Equilibrium Structure Determinations by Employing B3LYP/SNSD Anharmonic Force Fields: Validation and Application to Semirigid Organic Molecules,” J. Phys. Chem. A **119**, 2058–2082 (2015).

[63] É. Brémond, M. Savarese, N. Q. Su, Á. J. Pérez-Jiménez, X. Xu, J. C. Sancho-García, and C. Adamo, “Benchmarking Density Functionals on Structural Parameters of Small-/Medium-Sized Organic Molecules,” J. Chem. Theory Comput. **12**, 459–465 (2016).